AFRL-RX-TY-TP-2010-0089

MOTION OF LIQUID DORPLETS ON A SUPERHYDROPHOBIC OLEOPHOBIC SURFACT POSTPRINT

Hoon Joo Lee
North Carolina State University
Campus Box 7001
Raleigh, NC 27695-3742

Jeffery R. Owens
Airbase Technologies Division
Air Force Research Laboratory
139 Barnes Drive, Suite 2
Tyndall Air Force Base, FL 32403-5323

Contract No. FA8650-07-1-5916

August 2010

AIR FORCE RESEARCH LABORATORY
MATERIALS AND MANUFACTURING DIRECTORATE

■ **Air Force Materiel Command** ■ **United States Air Force** ■ **Tyndall Air Force Base, FL 32403-5323**

REPORT DOCUMENTATION PAGE

Form Approved
OMB No. 0704-0188

PLEASE DO NOT RETURN YOUR FORM TO THE ABOVE ADDRESS.

1. REPORT DATE *(DD-MM-YYYY)*	2. REPORT TYPE	3. DATES COVERED *(From - To)*
31-AUG-2010	Journal Article POSTPRINT	01-SEP-2009 -- 01-JUN-2010

4. TITLE AND SUBTITLE

Motion of Liquid Droplets on a Superhydrophobic Oleophobic Surface (POSTPRINT)

5a. CONTRACT NUMBER

FA8650-07-1-5916

5b. GRANT NUMBER

5c. PROGRAM ELEMENT NUMBER

0602102F

6. AUTHOR(S)

^Lee, Hoon Joo; *Owens, Jeffery R.

5d. PROJECT NUMBER

GOVT

5e. TASK NUMBER

L0

5f. WORK UNIT NUMBER

QL102006

7. PERFORMING ORGANIZATION NAME(S) AND ADDRESS(ES)

^North Carolina State University
Campus Box 7001
Raleigh, NC 27695-3742

8. PERFORMING ORGANIZATION REPORT NUMBER

9. SPONSORING/MONITORING AGENCY NAME(S) AND ADDRESS(ES)

*Air Force Research Laboratory
Materials and Manufacturing Directorate
Airbase Technologies Division
139 Barnes Drive, Suite 2
Tyndall Air Force Base, FL 32403-5323

10. SPONSOR/MONITOR'S ACRONYM(S)

AFRL/RXQL

11. SPONSOR/MONITOR'S REPORT NUMBER(S)

AFRL-RX-TY-TP-2010-0089

12. DISTRIBUTION/AVAILABILITY STATEMENT

Distribution Statement A: Approved for public release; distribution unlimited.

13. SUPPLEMENTARY NOTES

Published: J Mater Sci (2011) 46:69–76
Ref AFRL/RXQ Public Affairs Case # 10-110, 22 June 2010. Document contains color images.

14. ABSTRACT

Developing a superhydrophobic oleophobic material is achieved by two criteria: low surface energy and properly designed surface morphology. The relationships among surface tensions, contact angles, contact angle hystereses, roll-off angles, and surface morphologies of such materials are studied. Numerical formulae related to the surface energy of liquids and solids are used to predict the wetting behavior of superhydrophobic and oleophobic materials. Using chemical and geometrical modifications, a superhydrophobic oleophobic surface was prepared. Good agreement between the predicted and measured contact angles and roll-off angles were obtained. The effect of the contact angle hysteresis on the roll-off angle is described to understand the motion of a droplet when the droplet begins to roll off.

15. SUBJECT TERMS

contact angle, oleophobic, superhydrophobic, wetting

16. SECURITY CLASSIFICATION OF:			17. LIMITATION OF ABSTRACT	18. NUMBER OF PAGES	19a. NAME OF RESPONSIBLE PERSON
a. REPORT	b. ABSTRACT	c. THIS PAGE			Jeffery R. Owens
U	U	U	UU	8	19b. TELEPHONE NUMBER *(Include area code)*

Reset

Standard Form 298 (Rev. 8/98)
Prescribed by ANSI Std. Z39.18

J Mater Sci (2011) 46:69–76
DOI 10.1007/s10853-010-4810-z

Motion of liquid droplets on a superhydrophobic oleophobic surface

Hoon Joo Lee · Jeffery R. Owens

Received: 18 June 2010 / Accepted: 28 July 2010 / Published online: 10 August 2010

Abstract Developing a superhydrophobic oleophobic material is achieved by two criteria: low surface energy and properly designed surface morphology. The relationships among surface tensions, contact angles, contact angle hystereses, roll-off angles, and surface morphologies of such materials are studied. Numerical formulae related to the surface energy of liquids and solids are used to predict the wetting behavior of superhydrophobic and oleophobic materials. Using chemical and geometrical modifications, a superhydrophobic oleophobic surface was prepared. Good agreement between the predicted and measured contact angles and roll-off angles were obtained. The effect of the contact angle hysteresis on the roll-off angle is described to understand the motion of a droplet when the droplet begins to roll off.

Introduction

Wetting behavior of solid materials has recently gained a great deal of interest from both academia and industry [1–6]. This interest extends beyond the bio-inspired, lotus-leaf property of superhydrophobicity to materials that exhibit similar properties toward oils [7–10]. In this field, a surface with an oil contact angle over 90° is called an oleophobic surface, and a surface having a water contact angle exceeding 90° is defined as a hydrophobic surface. Although many researchers define a superhydrophobic surface as a surface having a water contact angle of greater than 150° and a roll-off angle of less than 5°, it should be noted that roll-off angles are strongly influenced by the mass of a water droplet [11, 12]. Therefore, we define a superhydrophobic surface as a surface with a water contact angle over 150°.

In this research, we study the relationships among surface tensions, surface morphologies, contact angles, contact angle hystereses, and roll-off angles on rough surfaces; propose numerical formulae related to the surface tension of liquids and solids to predict the wetting behavior of superhydrophobic and oleophobic materials; and create a nylon/cotton blended woven fabric (NyCo) which is superhydrophobic and highly oleophobic using chemical and geometrical modifications. We reduce the surface tension of the fibers by grafting a low-surface-energy material (LSEM) onto the fiber surface, by controlling the macro-scale roughness of the NyCo via the choice of yarn and fabric, and by employing micro- and nano-scale roughness on the fibers. Micro- and nano-scale roughness is achieved by allowing partial condensation of the LSEM before applying it to the NyCo, thus resulting in deposition of LSEM particulate condensates over the fiber surface. We also investigate the motion of water and oil droplets on a prepared NyCo when the surface was tilted and droplets began to roll off.

Design parameters for superhydrophobic oleophobic surface

The design of superhydrophobic oleophobic surfaces is predominantly informed by two rough wetting models: the Wenzel model and the Cassie–Baxter (CB) model. In the Wenzel model, a liquid fills the grooves of a rough surface, whereas in the CB model the liquid sits on top of

H. J. Lee (✉)
College of Textiles, North Carolina State University,
2401 Research Drive, Raleigh, NC 27695, USA
e-mail: hoonjoo_lee@ncsu.edu

J. R. Owens
Air Force Research Laboratory, RXQL, 139 Barnes Drive,
Building 1117, Tyndall Air Force Base, FL 32403, USA

the surface. As presented in our previous studies, the surface tension of a solid (γ_s) must be smaller than 6.35 dyne/cm to create a CB surface with an oil such as dodecane, which has a liquid surface tension (γ_L) of 24.5 dyne/cm [13]. However, since most solid surfaces possess γ_s >6.35 dyne/cm, the *metastable* CB model substitutes for the CB model. On a metastable CB surface, a liquid initially sits on top of the surface and is drawn into contact with the rough surface over time. An oleophobic surface can be produced by designing a metastable CB surface. A contact angle at a (metastable) CB rough surface can be described as

$$\cos\theta_r^{CB} = f_1 \cos\theta_e - f_2 \quad (1)$$

where θ_r^{CB} is an apparent contact angle on this surface, f_1 is the surface area of the liquid in contact with solid divided by the projected area, f_2 is the surface area of the liquid in contact with air divided by the projected area, and θ_e is the Young contact angle on a smooth surface [14]. Simply, if $f_2 = 0$ in Eq. 1, the rough surface is completely wet and $f_1 = r$, which is the roughness in the Wenzel model as

$$\cos\theta_r^{W} = r\cos\theta_e \quad (2)$$

where θ_r^{W} is an apparent contact angle on a Wenzel surface, and r is the ratio of the total wet area of a rough surface to the apparent surface area in contact with the water droplet [15]. According to Eq. 2, for a material with a smooth surface having $\theta_e = 120°$ for water, r must be greater than 1.79 to make the surface superhydrophobic, but the surface cannot be oleophobic since this rough surface will be filled by a liquid if θ_e <90°; i.e., a surface having θ_e <90° will become immediately wet (the Wenzel model), or eventually wet (the metastable CB model).

Experimental

Materials

Nylon 6,6 film (M_n: 12 kDa) and NyCo (50:50 nylon 6,6/cotton blended plain woven fabric) were used as smooth or rough surfaces, respectively. Heptadecafluoro-1,1,2,2-tetrahydrodecyltrimethoxysilane (fluorosilane, $C_{13}H_{13}F_{17}O_3Si$, Gelest, Morrisville, PA, USA), ammonium hydroxide (NH_4OH, Mallinckrodt Chemical, Raleigh, NC, USA), and isopropyl alcohol (C_3H_7OH, Fisher, Waltham, MA, USA) were used without further purification. Distilled water and dodecane ($C_{12}H_{26}$, Aldrich, St. Louis, MO, USA) were used as liquids to measure contact angles and roll-off angles.

Grafting of fluorosilane on nylon film and NyCo

In order to model a superhydrophobic oleophobic surface, Young contact angles, θ_e, of water and dodecane on a smooth surface covered by fluorosilane are required. Hence, fluorosilane was grafted to a nylon film. We added 1% ammonium hydroxide to a 4% fluorosilane solution in isopropyl alcohol and allowed partial condensation of the fluorosilane prior to treating the nylon film. A 0.5-g nylon film (10 × 10 cm^2) was immersed in the prepared solution, padded to remove excess liquid, and cured in a microwave oven (Panasonic NN-SD967S, Osaka, Japan) at 2.45 GHz/1.25 kW for three 30 s intervals alternated with 30 s cooling intervals. The fluorosilane-grafted nylon was rinsed in isopropyl alcohol and water for 2 h and air dried.

In the same manner, we added 1% ammonium hydroxide to 4% fluorosilane solution in isopropyl alcohol and allowed partial condensation of the fluorosilane prior to treating the NyCo. A 3.2-g NyCo fabric (10 × 10 cm^2) was immersed in the prepared solution, padded to remove excess liquid, and cured in a microwave oven at 2.45 GHz/1.25 kW for three 30 s intervals alternated with 30-s cooling intervals. The fluorosilane-grafted NyCo was rinsed in isopropyl alcohol and water for 2 h and air dried.

Scanning electron microscopy

The rough surface of NyCo fabric was examined with a scanning electron microscope (SEM, JEOL, 6400F, Tokyo, Japan) operated at 5 kV and magnifications from ×100 to ×20,000. Revolution™ (4pi Analysis, v1.60b24, Durham, NC, USA) was used for image analysis of SEM images. The fiber diameters and the distances between adjacent fibers were measured using this program.

Contact angle measurements

The contact angles of water and dodecane on the prepared surfaces were measured from sessile drops using a lab-designed goniometer at 20 °C. The volumes of the deposited droplets were 5 and 10 μL. The range of contact angles was obtained from at least three individual measurements each on a new spot. The image of liquid droplets on the prepared surface has been obtained using a digital camera (Canon, EOS EF-S-18-55IS, Lake Success, NY, USA) having an optical microscopic focusing lenses (Meiji Techno, EMZ-13TR, Saitama, Japan).

Roll-off angle measurements

The roll-off angles were measured by placing a specimen on a level platform mounted on a rotation stage (Newport, 495, Irvine, CA, USA) and inclining the stage. Water and dodecane droplets (50, 100, and 500 μL) were placed onto the surface, and the angle of the stage was recorded when the drops began to roll off. The image of liquid droplets on the surface has been obtained using a digital camera

(Canon, EOS EF-S-18-55IS), and measurements of advancing contact angles, receding contact angles, and contact angle hystereses were carried out.

Results and discussion

The wetting behavior of a solid surface is controlled by the chemical composition and the geometrical structure of the surface. We modified NyCo by grafting fluorosilane condensates over the fiber surface to generate a low-surface-tension surface. First, we verify that the chemical procedure described in "Experimental" section results in a low-surface-energy when the fluorosilane is grafted onto the substrate.

Chemical modification

We chemically grafted fluorosilane onto a nylon film and onto NyCo to reduce the surface tension and make the surface hydrophobic and *less oleophilic*. First, the Young contact angles, θ_e, of water and dodecane on a fluorosilane-grafted nylon film were measured since θ_e (water) and θ_e (dodecane) are important parameters to design a superhydrophobic and oleophobic surface using the Wenzel and the CB models. The water contact angles, θ_e (water), on a fluorosilane-grafted nylon film were 119°–124°, while θ_e (water) on an unmodified nylon surface were 70°–73°. Grafting fluorosilane to a nylon film also increased dodecane contact angles. The dodecane contact angles, θ_e (dodecane), on a fluorosilane-grafted nylon film were 73°–81°, while θ_e (dodecane) on an unmodified nylon surface was <5°. Fluorosilane grafted onto nylon film successfully generated a surface having low surface tension as shown in Fig. 1.

Geometrical modification

Again, to form a superhydrophobic oleophobic surface, two rough wetting models, the Wenzel and the CB models in Eqs. 1 and 2 are predominantly used. To obtain the real surface area we use a *flux integral*. As shown in Fig. 2, the distance from the center of a weft (or warp) yarn to the center of an adjacent weft (or warp) yarn is $4R$; and the distance from the center of a weft (or warp) yarn to the center of an adjacent warp (or weft) yarn is $2R$. Hence, according to Pythagorean theorem, the vector from the center of one weft yarn to the center of an adjacent weft yarn makes a 30° angle to the plane of the fabric.

Using the flux integral, the area of one yarn in the unit fabric is calculated as

$$r(u,v) = (2R + R\cos v)\cos ui + (2R + R\cos v)\sin uj + R\cos vk \tag{3}$$

$$r_u \times r_v = R(2R + R\cos v)\cos u\cos vi + R(2R + R\cos v)\sin u\cos vj + R(2R + R\cos v)\sin vk \tag{4}$$

$$|r_u \times r_v| = R(2R + R\cos v) \tag{5}$$

$$A_{\text{yarn in unit area}} = \frac{\int_0^{2\pi}\int_0^{2\pi} R(2R + R\cos v)\mathrm{d}u\mathrm{d}v}{3} \tag{6}$$

$$A_{\text{yarn in unit area}} = \frac{8\pi^2R^2}{3} = A_{\text{weft yarn in unit area}} = A_{\text{warp yarn in unit area}} \tag{7}$$

where R is the radius of yarn; A is the area; i, j, and k are the vectors to x-, y-, and z-axis direction, respectively; u and v are the notations for the variables of integration. Then, we determine the true fabric surface area as follows:

$$A_{\text{fabric}}^{\text{real}} = A_{\text{weft yarn in unit area}} + A_{\text{warp yarn in unit area}} = 52.64R^2 \tag{8}$$

where $A_{\text{fabric}}^{\text{real}}$ is the intrinsic area of the unit fabric determined by the area of yarn surfaces. The apparent surface area is just equal to the area of a plane tangent to the top surface.

$$A_{\text{fabric}}^{\text{apparent}} = 2\sqrt{3}R \times 2\sqrt{3}R = 12R^2 \tag{9}$$

where $A_{\text{fabric}}^{\text{apparent}}$ is the apparent area of the unit fabric shown in Fig. 2. Finally, the roughness, r, is just the ratio of these areas

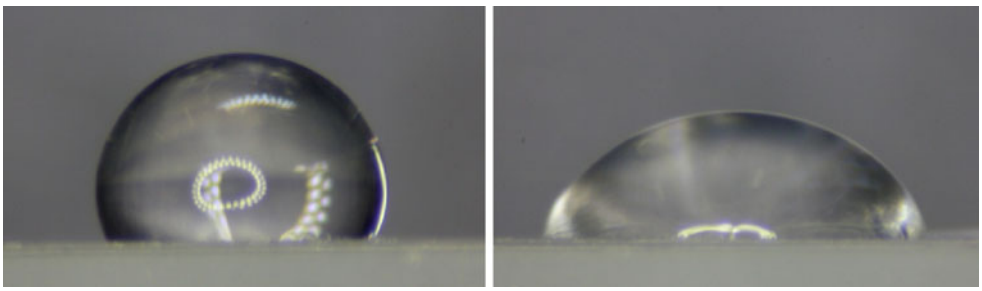

Fig. 1 10 μL water and dodecane droplets on a fluorosilane-grafted nylon film

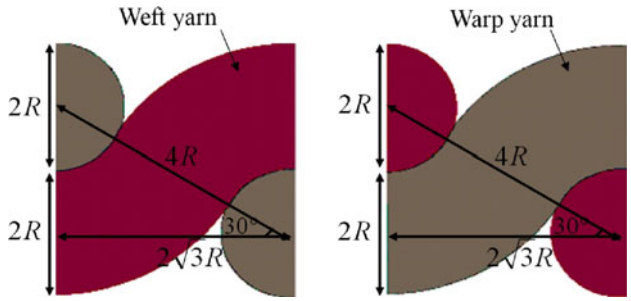

Fig. 2 Cross-section views of a plain woven fabric

$$r = \frac{A_{\text{fabric}}^{\text{real}}}{A_{\text{fabric}}^{\text{apparent}}} = \frac{52.64R^2}{12R^2} = 4.39 \tag{10}$$

As shown in Eq. 10, the plain woven rough surface has high enough r to achieve a metastable CB surface. Next, we look at a plain woven fabric made with multifilament yarns. Clearly, a multifilament yarn will have even higher values of r, because the space between the fibers will increase the real surface area while the apparent surface area remains the same. In this case, Eq. 8 becomes

$$A_{\text{fabric}}^{\text{real}} = A_{\text{multi}} \approx 52.64R \times NR_{\text{f}} \tag{11}$$

where N is the number of filament fibers, R is the radius of the yarn, and R_{f} is the radius of the filament fibers. Substituting Eq. 11 into 10 yields

$$r = \frac{A_{\text{fabric}}^{\text{real}}}{A_{\text{fabric}}^{\text{apparent}}} = 4.39\frac{NR_{\text{f}}}{R} \tag{12}$$

Now, we model a CB plain woven fabric. In Fig. 2, the center-to-center distance is $2\sqrt{3}R$ and the contact angle on a CB NyCo surface, $\theta_{\text{r}}^{\text{CB}}$, is defined as

$$\cos\theta_{\text{r}}^{\text{CB}} = \frac{(\pi - \theta_{\text{e}})}{\sqrt{3}}\cos\theta_{\text{e}} + \frac{\sin\theta_{\text{e}}}{\sqrt{3}} - 1 \tag{13}$$

Substituting Young contact angles into Eq. 13 along with the measured contact angles from the flat nylon film provides $\theta_{\text{r}}^{\text{CB}}$. Meanwhile, we obtained $d_{\text{f}} \sim 1.5R_{\text{f}}$, where R_{f} is the fiber radius and $2d_{\text{f}}$ is the distance between two adjacent fibers, by analyzing SEM images with Revolution™ v1.60b24 (Fig. 3). Therefore, the contact angle on CB multi-filament fibers, $\theta_{\text{r}}^{\text{multifilament}}$, is defined as:

$$\cos\theta_{\text{r}}^{\text{multifilament}} = \frac{2(\pi - \theta_{\text{e}})}{5}\cos\theta_{\text{e}} + \frac{2\sin\theta_{\text{e}}}{5} - 1 \tag{14}$$

Substituting $119° \le \theta_{\text{e}}$ (water) $\le 124°$ and $73° \le \theta_{\text{e}}$ (dodecane) $\le 81°$ into Eq. 13, we find $142° \le \theta_{\text{r}}^{\text{CB}}$ (water) $\le 147°$ and $98° \le \theta_{\text{r}}^{\text{CB}}$ (dodecane) $\le 106°$ for the fluorosilane-grafted plain woven fabric. In the same manner, substituting the same θ_{e} into Eq. 14, we obtain $149° \le \theta_{\text{r}}^{\text{multifilament}}$ (water) $\le 152°$ and $114° \le \theta_{\text{r}}^{\text{multifilament}}$ (dodecane) $\le 120°$ for the fluorosilane-grafted multifilament yarns. Using these values as the effective contact angles for the yarns in the woven structure and re-solving Eq. 13, i.e., substituting these values into θ_{e} (water) and θ_{e} (dodecane) in Eq. 13, we predict $166° \le \theta_{\text{r}}^{\text{CB}}$ (water) $\le 168°$ and $138° \le \theta_{\text{r}}^{\text{CB}}$ (dodecane) $\le 143°$ for the fluorosilane-grafted multifilament plain woven fabric. According to our prediction, NyCo multifilament plain woven fabric can be superhydrophobic and oleophobic once the fabric is treated with an LSTM. Figure 4 shows water and dodecane droplets on the fluorosilane-grafted NyCo; the initial apparent contact angles of water and dodecane on this surface are $162° \le \theta_{\text{r}}^{\text{CB}}$ (water) $\le 171°$ and $139° \le \theta_{\text{r}}^{\text{CB}}$ (dodecane) $\le 143°$; and both droplets are sitting on top of the rough surface. However, dodecane is slowly drawn into the woven structure with reducing $\theta_{\text{r}}^{\text{CB}}$ (dodecane) while water stays on top of the surface until water completely evaporates. Good agreement between the predicted and measured contact angles was obtained.

Contact angle hystereses and roll-off angles

A liquid droplet on a tilted surface can stay or roll off. A water or oil droplet rolls off a hydrophobic or oleophobic surface easier than from a hydrophilic or oleophilic surface. When a droplet begins to roll off, the advancing contact angle reaches 180° while the receding contact angle varies and depends on the local structure of the solid surface and the surface energy of the liquid and the solid. For our fluorosilane-grafted NyCo fabric, the advancing contact angles of both water and oil approached 180° when the droplet began to move, but the receding contact angles varied depending on the surface tension of the liquid. In addition, it is important to note that the roll-off angle is also strongly influenced by the volume of the droplet, as shown in Eq. 15.

$$mg\sin\alpha = -D\gamma_{\text{L}}(\cos\theta_{\text{A}} - \cos\theta_{\text{R}}) \tag{15}$$

where m is the mass of the droplet, g is the gravitational acceleration, α is the roll-off angle, γ_{L} is the liquid surface tension, D is the diameter of the wetting area, θ_{A} is the advancing contact angle, and θ_{R} is the receding contact angle. A droplet cannot roll off if the size of the droplet is smaller than that of the underlying structure of a rough surface. On the other hand, although a receding contact angle is smaller than 90°, the roll-off angle can be less than 5° if a very large droplet is deposited on a surface and the surface is inclined. Therefore, it is important to understand the relationship between the volume of a liquid droplet and the diameter of the wetting area of a solid when the liquid is deposited on a surface. In the limit of small droplets, a drop deposited on a solid surface can have a nearly spherical cap with a circular contact line as shown in Fig. 5.

The radius of the wetting area, R_D, on a surface having a contact angle no greater than 90° is

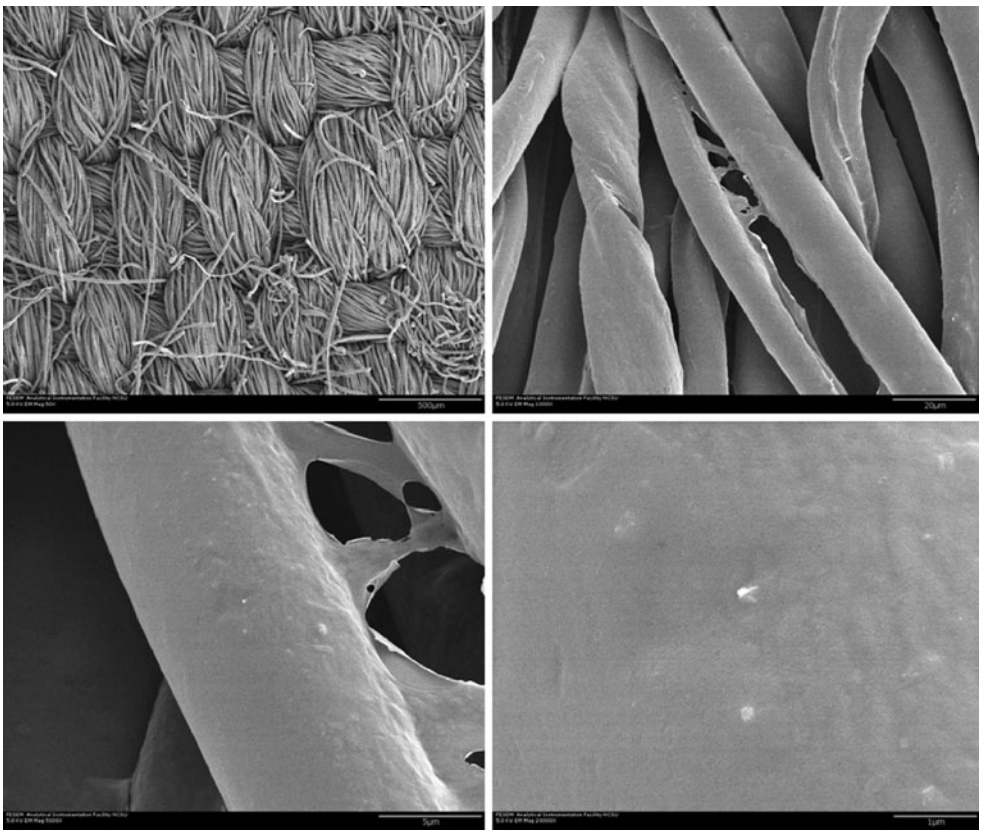

Fig. 3 SEM images of NyCo multifilament plain woven structures (×50, 1 K, 5 K, and 20 K)

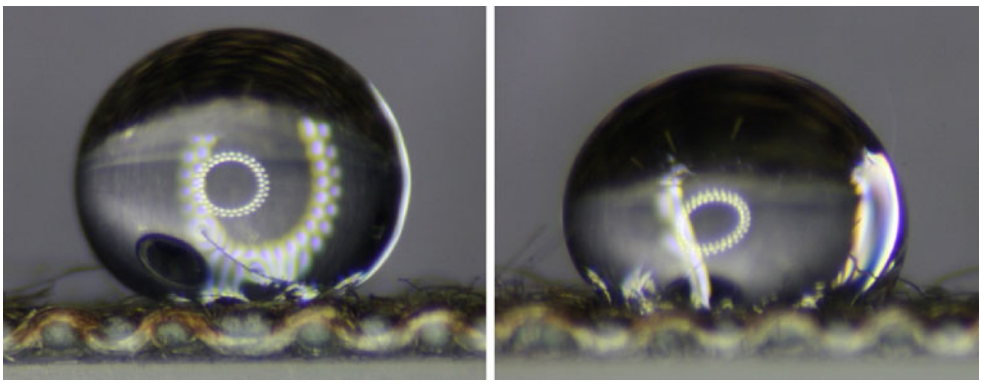

Fig. 4 10 μL water and dodecane droplets on a fluorosilane-grafted NyCo

$$R_{\mathrm{D}} = \sqrt[3]{\frac{3V}{\pi(2 - 3\cos\theta + \cos^3\theta)}} \tag{16}$$

where V is the volume of the liquid and θ is the contact angle. However, if θ is no smaller than 90°, R_D is

$$R_{\mathrm{D}} = \sqrt[3]{\frac{V}{\frac{4\theta}{3\sin^3\theta} + \frac{\pi}{3\tan(\pi-\theta)}}} \tag{17}$$

Since $D = 2R_{\mathrm{D}}$, the diameter of the wetting area can be predicted as shown in Table 1.

Because advancing contact angles are close to 180° when droplets begin to move, the values of receding contact angles are required to predict roll-off angles. A receding contact angle can be predicted by computing contact angle hystereses, θ_{H}, which is the difference between θ_{A} and θ_{R}, McHale visualized the relationship between the contact angle hysteresis of a smooth surface and that of a rough surface by developing a *gain factor*, which is the variation rate of the contact angle hysteresis when a surface is roughened [16]. As two predominant rough wetting models (the Wenzel and the CB models) are

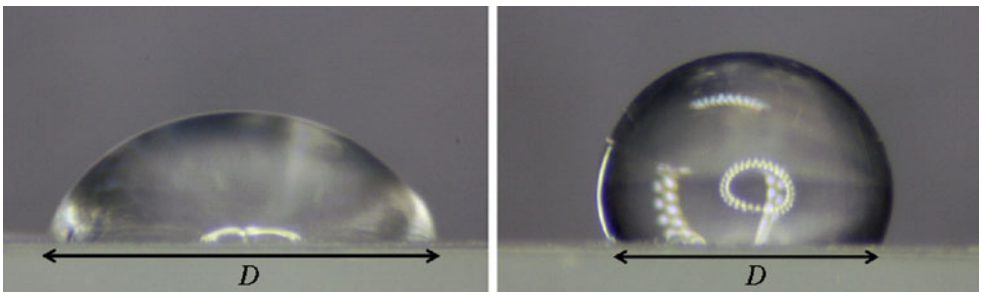

Fig. 5 The diameter of wetting area, D, of 10 μL of a liquid on a surface having $\theta \leq 90°$ and $\theta \geq 90°$

Table 1 Diameter of wetting area of liquid droplets

θ (°)	D (mm)			
	5 μL	10 μL	20 μL	50 μL
10	38.13	48.04	60.53	82.15
20	15.29	19.26	24.27	32.94
30	9.06	11.41	14.37	19.51
40	6.32	7.96	10.03	13.61
50	4.84	6.10	7.68	10.42
60	3.94	4.96	6.25	8.49
70	3.35	4.22	5.32	7.22
80	2.95	3.72	4.69	6.36
90	2.67	3.37	4.24	5.76
100	2.48	3.13	3.94	5.34
110	2.26	2.85	3.59	4.87
120	2.01	2.54	3.20	4.34
130	1.74	2.19	2.76	3.75
140	1.44	1.81	2.28	3.09
150	1.10	1.39	1.75	2.38
160	0.75	0.94	1.19	1.61
170	0.37	0.47	0.59	0.81

commonly used to understand the wetting behavior of a rough surface, two kinds of gain factors can be presented: the Wenzel gain factor, G_r^W, and the CB gain factor, G_r^{CB}. Here, G_r^W and G_r^{CB} are determined as

$$G_r^W = \frac{\delta(r\cos\theta_e)}{\delta(\cos\theta_r^W)} = \frac{r\sin\theta_e}{\sin\theta_r^W} \tag{18}$$

$$G_r^{CB} = \frac{\delta(f\cos\theta_e)}{\delta(\cos\theta_r^{CB})} = \frac{f\sin\theta_e}{\sin\theta_r^{CB}} \tag{19}$$

where f is the fraction of the projected area of a solid surface in contact with a liquid ($f = 1 - f_2$). The Wenzel equation provides a change in the contact angle hysteresis on a Wenzel rough surface, $\Delta\theta_H^W$, caused by a change in the contact angle hysteresis on a smooth surface, $\Delta\theta_H$, as

$$\Delta\theta_H^W = G_r^W\Delta\theta_H = \frac{r\sin\theta_e}{\sin\theta_r^W}\Delta\theta_H \tag{20}$$

When a contact angle θ_e is close to 90°, $\Delta\theta_H^W$ has approximately the same value as $\Delta\theta_H$. However, since the effect of roughness is proportional to the sine value of $\Delta\theta_H$, $\Delta\theta_H^W$ rapidly increases as r increases. Likewise, the CB equation provides a change in the contact angle hysteresis on a CB rough surface, $\Delta\theta_H^{CB}$, caused by a change in the contact angle hysteresis on a smooth surface, $\Delta\theta_H$, as

$$\Delta\theta_H^{CB} = G_r^{CB}\Delta\theta_H = \frac{f\sin\theta_e}{\sin\theta_r^{CB}}\Delta\theta_H \tag{21}$$

Since f varies from 1 to ~0 when a surface is roughened, $\Delta\theta_H^{CB}$ is always smaller than $\Delta\theta_H$ on a rough surface and decreases as f_2 increases. As a numerical example, if a water droplet is deposited on a nylon rough surface having $\theta_e = 70°$, $\Delta\theta_H = 110°$ and $r = 3$, the apparent contact angle, θ_r^W, will be ~0° and thus the contact angle hysteresis on this Wenzel surface, $\Delta\theta_H^W$, will be over 90°, i.e., the droplet will be adsorbed onto the rough structure and will not be able to roll off such a hydrophilic rough surface. However, if a water droplet is deposited on a poly(tetrafluoroethylene) (PTFE) having $\theta_e = 120°$, $\Delta\theta_H = 90°$ and $f = 0.26$, the apparent contact angle, θ_r^{CB}, will be 150° and thus the contact angle hysteresis, $\Delta\theta_H^{CB}$, on this CB surface will be 45°, i.e., the surface will become superhydrophobic and the droplet rolls readily off the surface at a certain inclination angle.

The roll-off angles of water and dodecane were predicted and compared with the measured values. Table 2 shows the predicted roll-off angles, α, of 50 and 100 μL droplets of water and dodecane on fluorosilane-grafted NyCo. For water, α can be simply predicted by substituting D, obtained using Eq. 17, and $\Delta\theta_H^{CB}$, carried out from Eqs. 19 and 21, into Eq. 15 since $\theta_R^{CB} = \theta_A^{CB} - \Delta\theta_H^{CB}$. However, in this study, a measured D is used instead of the predicted D since the shape of a liquid droplet is not perfectly spherical when $V \geq 10$ μL.

Table 2 Predicted roll-off angles of water and dodecane on fluorosilane-grafted NyCo

Parameters	Water (γ_L = 72.8 dyne/cm)		Dodecane (γ_L = 24.5 dyne/cm)	
	50 μL	100 μL	50 μL	100 μL
min θ_e (°)[a]	119	119	73	73
$\Delta\theta_H$ (°)[a]	151	151	168	168
f	0.18	0.18	0.18	0.18
min θ_r^{CB} (°)[b]	162	162	139	139
$\Delta\theta_H^{CB}$ (°)[b]	76	76	156	156
θ_A^{CB} (°)[b]	180	180	180	180
θ_R^{CB} (°)[b]	103	103	25	25
D (mm)[a]	5	6.5	7.5	9
m (mg)	50	100	50	100
α (°)	35	22	46	25

[a] Measured values

[b] For both stable and metastable CB surfaces

In the case of dodecane, whose $\theta_e < 90°$ and $\theta_r^{CB} > 90°$, the situation is less favorable, and Eqs. 19 and 21 cannot be used to predict α of dodecane since the sine curve has a bilateral symmetry with respect to 90°. Hence, Eqs. 19 and 21 have to be modified for a metastable CB surface as below.

$$G_r^{\text{meta-CB}} = \frac{f(1+\cos\theta_e)}{(1+\cos\theta_r^{CB})} \tag{22}$$

$$\Delta\theta_H^{\text{meta-CB}} = G_r^{\text{meta-CB}}\Delta\theta_H = \frac{f(1+\cos\theta_e)}{(1+\cos\theta_r^{CB})}\Delta\theta_H \tag{23}$$

Therefore, for dodecane, α can be predicted by substituting D and $\Delta\theta_H^{\text{meta-CB}}$ into Eq. 15. The respective predicted values of α are 35° and 22° for 50 and 100 μL water droplets, and 46° and 25° for 50 and 100 μL dodecane droplets, as shown in Table 2. Meanwhile, 100 μL water and dodecane droplets were deposited on the prepared fluorosilane-grafted NyCo woven fabric and the surface was steadily inclined to measure the roll-off angles of this superhydrophobic oleophobic surface. As shown in Fig. 6, the measured α of water and dodecane are 18.5° and 20°, respectively; these numbers are very close to the values predicted in Table 2. Again, if liquids having different γ_L are deposited on a solid surface, the roll-off angles of the liquids are strongly influenced by the size and the surface energy of each liquid.

Conclusion

In this research, the wetting behavior of a flat surface was compared with that of a rough surface. A superhydrophobic oleophobic surface has been obtained by two criteria: low surface tension and a proper surface roughness. To make NyCo superhydrophobic and oleophobic, NyCo plain woven fabric consisting of multifilament yarns was treated with fluorosilane, which has a very low surface tension, through a microwave-promoted reaction. From the Young contact angles of water and dodecane on a fluorosilane-grafted nylon film, we predicted the apparent contact angles on a fluorosilane-grafted NyCo fabric. The effect of the size and the contact angle hysteresis of water and dodecane droplets on such a superhydrophobic oleophobic rough surface was analyzed, and the shape and the motion of the droplets were studied to understand the wetting behavior of both stable and metastable CB surfaces. To make a droplet roll off at a very shallow inclination angle,

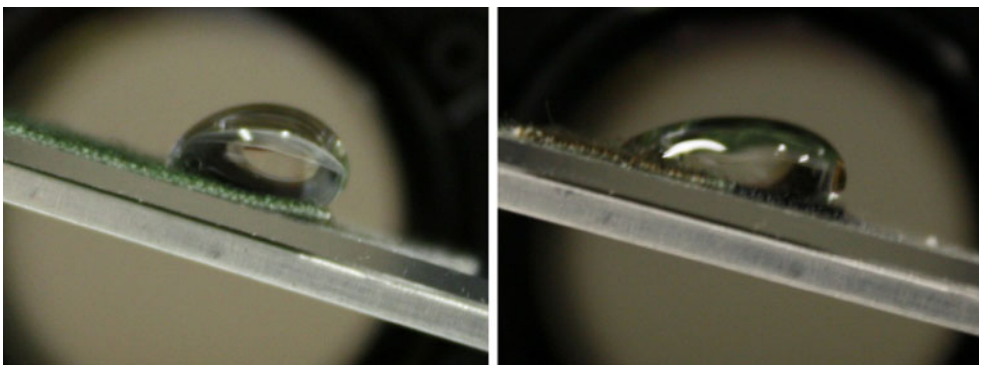

Fig. 6 100 μL water and dodecane droplets on a tilted fluorosilane-grafted NyCo just before rolling off

the contact angle hysteresis should be small. For hydrophobic and oleophobic surfaces, stable and metastable CB gain factors are the attenuation of contact angle hystereses. Good agreement between the predicted values and the measured values of contact angles and roll-off angles was obtained. It is important to note that the form of the CB gain factor (Eq. 19) should be modified to the metastable CB gain factor (Eq. 22) to predict a receding contact angle of an oil droplet on an oleophobic rough surface.

Acknowledgements This material was sponsored by the Air Force Research Laboratory (AFRL) under grant number FA8650-07-1-5903. The U.S. Government is authorized to reproduce and distribute reprints for Governmental purposes notwithstanding any copyright notation thereon. We also appreciate support from the Defense Threat Reduction Agency-Joint Science and Technology Office for Chemical and Biological Defense (grant number HDTRA1-08-1-0049) and US Army Natick Soldier Research Development and Engineering Center (NSRDEC).

References

1. Cai Y, Li Q, Wei Q, Wu Y, Song L, Hu Y (2008) J Mater Sci 43:6132. doi:10.1007/s10853-008-2921-6
2. Lee B, Dai G (2009) J Mater Sci 44:4848. doi:10.1007/s10853-009-3739-6
3. Pascual M, Balart R, Sanchez L, Fenollar O, Calvo O (2008) J Mater Sci 43:4901. doi:10.1007/s10853-008-2712-0
4. Berketis K, Tzetzis D (2009) J Mater Sci 44:3578. doi:10.1007/s10853-009-3485-9s
5. Huang X, Fang X, Lu Z, Chen S (2009) J Mater Sci 44:4522. doi:10.1007/s10853-009-3660-z
6. Lee HJ (2009) J Mater Sci 44:4645. doi:10.1007/s10853-009-3711-5
7. Ahuja A, Taylor JA, Lifton V, Sidorenko AA, Salamon TR, Lobaton EJ, Kolodner P, Krupenkin TN (2008) Langmuir 24:9
8. Steele A, Bayer I, Loth E (2009) Nano Lett 9:501
9. Tuteja A, Choi W, Mabry JM, McKinley GH, Cohen RE (2008) Proc Natl Acad Sci USA 105:18200
10. Lee HJ, Willis C (2009) Chem Ind 21
11. Michielsen S, Lee HJ (2007) Langmuir 23:6004
12. Leng B, Shao Z, de With G, Ming W (2009) Langmuir 25:2456
13. Lee H, Owens J (2010) J Mater Sci 45:3247. doi:10.1007/s10853-010-4332-8
14. Cassie ABD, Baxter S (1944) Trans Faraday Soc 40:546
15. Wenzel RN (1936) Ind Eng Chem 28:988
16. McHale G, Shirtcliffe N, Newton M (2004) Langmuir 20:10146